1. Extended Data

Figure #	Figure title One sentence only	Filename This should be the name the file is saved as when it is uploaded to our system. Please include the file extension. i.e.: *Smith_ED_Fig1.jpg*	Figure Legend If you are citing a reference for the first time in these legends, please include all new references in the main text Methods References section, and carry on the numbering from the main References section of the paper. If your paper does not have a Methods section, include all new references at the end of the main Reference list.
Extended Data Fig. 1	A comparison of BET surface areas and total pore volumes of sonoCOFs synthesized in aqueous and organic solvents.	Extended_Figure_1.pdf	The Brunauer–Emmett–Teller (BET) surface area (dark shading) and pore volume (light shading) of all the synthesized sonoCOFs in aqueous solvent (blue bars) are greater than or equal to the equivalent synthesized in organic solvent (pink bars).

2. Supplementary Information:

A. Flat Files

Item	Present?	Filename This should be the name the file is saved as when it is uploaded to our system, and should include the file extension. The extension must be	A brief, numerical description of file contents. i.e.: *Supplementary Figures 1-4, Supplementary Discussion, and Supplementary Tables 1-4.*

		.pdf	
Supplementary Information	Yes	NATSYNTH-21060062-Wu-SI.pdf	Supplementary Text, Supplementary Figs 1-127, Supplementary Tables 1-14.
Reporting Summary	No		
Peer Review Information	No	*OFFICE USE ONLY*	

B. Additional Supplementary Files

Type	Number If there are multiple files of the same type this should be the numerical indicator. i.e. "1" for Video 1, "2" for Video 2, etc.	Filename This should be the name the file is saved as when it is uploaded to our system, and should include the file extension. i.e.: *Smith_ Supplementary_Video_1.mov*	Legend or Descriptive Caption Describe the contents of the file
Choose an item.			

3. Source Data

Parent Figure or Table	Filename This should be the name the file is saved as when it is uploaded to our system, and should include the file extension. i.e.: *Smith_SourceData_Fig1.xls,* or *Smith_ Unmodified_Gels_Fig1.pdf*	Data description i.e.: Unprocessed Western Blots and/or gels, Statistical Source Data, etc.
Source Data Extended Data Fig. 1	Source_data_ED_Fig_1.xlsx	Raw data for Extended Data Fig. 1

Source Data Fig. 5a, 5b	Source_data_Fig_5a_5b.xlsx	Raw data for Fig. 5a,b
Source Data Fig. 5d, 5e	Source_data_Fig_5d_5e.pdf	Full-size TEM images supporting Fig. 5d,e

Using sound to synthesize covalent organic frameworks in water

Wei Zhao[1, 2], Peiyao Yan[1], Haofan Yang[1, 2], Mounib Bahri[3], Alex M. James[1], Hongmei Chen[1], Lunjie Liu[1], Boyu Li[1], Zhongfu Pang[1, 2], Rob Clowes[1], Nigel D. Browning[3], John W. Ward*[1, 2], Yue Wu*[1] and Andrew I. Cooper*[1, 2]

Covalent organic frameworks (COFs) are typically synthesized using solvothermal conditions (>120 °C, >72 h) in harmful organic solvents. Here, we report a strategy for rapidly (< 60 min) synthesizing imine-linked COFs in aqueous acetic acid using sonochemistry and thus avoid most of the disadvantages of solvothermal methods. Using the sonochemical method, we synthesize seven known COFs. The crystallinity and porosity of these COFs is comparable with or better than the same materials made by established solvothermal routes. The sonochemical method even works in sustainable solvents, such as food-grade vinegar. The generality of the method is shown in the preparation of two previously unreported COFs. Finally, a COF synthesized sonochemically acts as an excellent photocatalyst for sacrificial hydrogen evolution from water, showing a more sustained catalytic performance compared with its solvothermal analog. The speed, ease and generality of this sonochemical method together with improved material quality makes the use of sound an enabling methodology for the rapid discovery of functional COFs.

Crystalline covalent organic frameworks (COFs) have received much attention because of their use in catalysis, adsorption, separation, chemo-sensing, drug delivery, and energy storage and production.[1-3] The traditional route to COFs is solvothermal synthesis,[4] but this often requires the use of sealed, pressurized tubes, elevated reaction temperatures (120–200 °C), long reaction times (2–7 days) and toxic organic solvents. These drawbacks provide an incentive to develop alternative methods to synthesize COFs.

Alternatives to solvothermal syntheses include microwave synthesis[5] and room-temperature syntheses using catalysts.[6,7] These routes can be much faster than solvothermal syntheses, with reaction times of 1-2 hours. However, it is still desirable to avoid the use of toxic organic solvents and metal catalysts. Solid-state synthesis is one route that eliminates bulk solvent use and reduces waste generation. *p*-Toluenesulfonic acid (PTSA), a strong solid acid, was first used as the catalyst for solid-state COF synthesis by Kandambeth *et al*..[8] However, a large quantity of PTSA (~6 molar equivalents based on the amine monomers) was required during the synthesis, and high temperatures (90–170 °C) for 1 minute to 2 days were needed to obtain the crystalline COFs. [9,10] Mechanochemical synthesis is another promising solid-state route. The first examples of COF mechanosynthesis were reported by Biswal *et al*.[11] Solvent-free mechanochemical processes offer the potential for large-scale COF synthesis but such studies are rare and the COFs produced have limited crystallinity and porosity.[12] For example, the mechanically synthesized COFs, TpPa-1, TpPa-2, and TpBD, had only moderate crystallinity and low Brunauer-Emmet-Teller (BET) surface areas (61 $m^2 g^{-1}$ for TpPa-1, 56 $m^2 g^{-1}$ for TpPa-2, and 35 $m^2 g^{-1}$ for TpBD) compared to their solvothermal analogs.[11] Recent work by Emmerling *et al*.[13] showed that alternative activation methods such as supercritical CO_2 drying[14,15] may allow access to the porosity of mechanochemically prepared COFs.

Aqueous COF synthesis is attractive because it avoids the use of organic solvents. There are a limited number of reports of keto-enamine-based and azine-linked COFs produced using hydrothermal syntheses,[16,17] but long reaction times (0.5–3 days) and elevated temperatures (>120 °C) were still required in the examples reported. Moreover, the authors concluded that their method only works well for COFs that are stabilized by keto-enol tautomerism, because conventional imine bonds are susceptible to the reversible back reaction upon exposure to water. Recently, Martín-Illán *et al*. developed a protocol for the aqueous synthesis of imine-linked COFs at 80 °C for 5 days.[18] However, a very low concentration of starting monomers was required owing to their low aqueous solubility and an organic solvent (DMSO) was used to aid solubilization in some cases. Even when microwave radiation was used to accelerate the reaction, a 5-hour reaction time was still needed to obtain the COF.

Sonochemical reactions are driven by high-energy ultrasound. In sonochemistry, acoustic cavitation occurs because of the formation, growth, and implosive collapse of bubbles in a liquid due to ultrasonic shearing. This cavitation produces localized hot spots that can accelerate reactions.[19] One advantage of sonochemistry is that the equipment required—an ultrasonic probe (Fig. 1)—is compact, easy to use, relatively inexpensive (around the cost of a basic rotary evaporator) and amenable to small-scale discovery chemistry. To our knowledge, the only reports of sonochemical COF synthesis are by Yang and co-workers[20] and by Yoo *et al*.[21] In those studies, first-generation COFs based on the less stable boroxine chemistry were prepared. Here, we focus on the stable, functional COFs synthesized *via* imine condensation that are the focus of much current research.

[1] Materials Innovation Factory and Department of Chemistry, University of Liverpool, Crown Street, Liverpool L69 7ZD, UK; [2] Leverhulme Research Centre for Functional Materials Design, Materials Innovation Factory and Department of Chemistry, University of Liverpool, Liverpool, UK; [3] Albert Crewe Centre for Electron Microscopy, University of Liverpool, Liverpool, L69 3GL, UK. Email: john.ward@liverpool.ac.uk, yue.wu@liverpool.ac.uk, aicooper@liverpool.ac.uk

We present a strategy for the sonochemical synthesis of imine-linked COFs in aqueous acetic acid. The reaction times are very short and the resultant materials often have superior properties to the same COFs obtained using other synthetic procedures. To thoroughly test this approach, we report the preparation of seven known COFs[22-27] and two new COFs. These 'sonoCOFs' are prepared in less than 1 hour with high crystallinity and porosity levels that are comparable to, or better than, COFs formed by solvothermal methods. Hazardous organic solvents are avoided, making the method safer, cleaner, more economical and simpler. We also tested the functional performance of the sonoCOFs against solvothermal COFs for sacrificial photocatalytic H_2 evolution. Several COFs prepared by the sonochemical method had excellent photocatalytic performance; in particular, sonoCOF-3 showed better sustained hydrogen evolution over 40 hours than its solvothermal analog.

Results and discussion

Sonochemical synthesis of a prototypical COF. To test our hypothesis that sonochemical synthesis may be feasible for imine-linked COFs, we chose a prototypical imine-linked COF known as "TAPB-DMTA COF", formed from the condensation of 1,3,5-tris(4-aminophenyl)benzene (TAPB) and 2,5-dimethoxybenzene-1,4-dicarboxaldehyde (DMTA), and known for its stability and crystallinity.[22] We discovered that this COF was easily synthesized through the ultrasonic irradiation of a dispersion of amine and aldehyde linkers in 6 M aqueous acetic acid (AcOH) without the need for any other organic solvents. We therefore selected this COF (Figure 2a, referred to here as sonoCOF-1) as a model system to explore the synthetic conditions in more detail. Unless otherwise stated, all of the sonochemical reactions were performed with a 550 W ultrasonic probe in continuous mode using a 3 mm microtip probe at 50% sonication power (the maximum recommended power for the probe used).

We first investigated the effect of reaction time on product quality and yield. Reactions were run for 5, 10, 30 and 60 min. The formation of sonoCOF-1 was confirmed by powder X-ray diffraction (PXRD) and Fourier-transform infrared (FT-IR) spectroscopy (Figure 2b and 2d). SonoCOF-1 was produced in 38 % yield after just 5 minutes sonication. Yields increased rapidly with reaction time: 76 % for 10 min, 93 % for 30 min and 93 % for 60 min (Figure 2e). Experiments for 60 min at sonication powers of 10–50 % in 10 % intervals showed lower yields at lower power but high crystallinity in all cases (Supplementary Fig. 21 and Supplementary Table 3).

The permanent porosity of sonoCOF-1 was assessed by nitrogen adsorption isotherms measured at 77 K. Longer sonication times led to an increase in BET surface area and total pore volume, reaching a maximum of 2059 $m^2 g^{-1}$ and 1.80 $cm^3 g^{-1}$, respectively, after 60 minutes (insufficient sample was obtained for reliable measurements from the 5-minute reaction) (Fig. 2c, Fig. 2e). Longer reaction times (90 and 120 min) showed little further change (Supplementary Fig. 44). Among the conditions tested, 1 hour was found to be the optimal reaction time for the formation of sonoCOF-1, which is much faster than the 72 hours commonly used for the solvothermal reaction.[22]

We also studied the effect of AcOH concentration on the formation of sonoCOF-1. PXRD analysis (Supplementary Fig. 20) showed that crystalline sonoCOF-1 could also be formed in 1 M and 3 M aqueous AcOH, but lower BET surface areas (261 $m^2 g^{-1}$ for 1 M and 1392 $m^2 g^{-1}$ for 3 M) and smaller pore volumes (0.22 $cm^3 g^{-1}$ for 1 M and 1.11 $cm^3 g^{-1}$ for 3 M) were obtained. SonoCOF-1 could even be prepared using food-grade distilled vinegar (~1M AcOH) giving a BET surface area of 380 $m^2 g^{-1}$ and pore volume of 0.32 $cm^3 g^{-1}$. Finally, we investigated the possibility of scaling up the reaction. We found that a 10× scale reaction using a 1.27 cm (1/2 inch) diameter probe at 100 % sonication power gave a good yield (73 %) and the BET surface area (2008 $m^2 g^{-1}$) and crystallinity were comparable to the equivalent small-scale reactions.

Scope of the aqueous sonochemical method. To demonstrate the generality of our aqueous sonochemical strategy, we synthesized a diverse set of 6 more known COFs that were prepared previously using solvothermal methods: sonoCOF-2 ('COF-JLU5')[23] composed of 4,4',4''-(1,3,5-triazine-2,4,6-triyl)trianiline (TAPT) and DMTA, sonoCOF-3 ('TPT-COF-4')[27] composed of TAPT and tris(4-formylphenyl)amine (TFPA), sonoCOF-4 ('N3-COF')[25] composed of TAPT and 1,3,5-triformylbenzene (TFB), sonoCOF-5 ('Py-1P COF')[28] composed of 4,4',4'',4'''-(pyrene-1,3,6,8-tetrayl)tetraaniline (PTTA) and terephthalaldehyde (TPA), sonoCOF-6 ('RT-COF-1')[29] composed of TAPB and TPA, and sonoCOF-7 ('COF-432')[24] composed of 4,4',4'',4'''-(ethene-1,1,2,2-tetrayl)tetraaniline (ETTA) and TFB (Supplementary Table 1). The corresponding sonoCOF-x (os, 'organic solvent', x = 2–7) series was also synthesized in mixtures of 1,4-dioxane/mesitylene or n-BuOH/o-DCB as a control (details in Supplementary Information section 2.2). The identities of the sonoCOF reaction products were confirmed by elemental analysis, FT-IR spectroscopy, thermogravimetric analysis (TGA), PXRD, and N_2 sorption analysis.

All sonoCOFs exhibited good crystallinities as gauged by PXRD. By contrast, not all sonoCOFs could be prepared as crystalline products in the organic solvents we tested; for example, sonoCOF-3 (os) and sonoCOF-7 (os) were almost amorphous (Supplementary Fig. 23). These results suggest that the aqueous sonochemical synthesis of imine COFs may be more robust than equivalent syntheses in organic solvents. As shown in Figure 3, the experimental PXRD patterns of sonoCOF-1–7 are consistent with the structures reported in the literature. The unit cell parameters of sonoCOF-1–7 were refined by the Pawley method (Supplementary Tables 3–9). We note that sonoCOF-3 shows an unassigned peak at around 5.6 °, which was also observed in other reports[27,40].This peak is thought to arise from stacking faults. Scanning electron microscopy (SEM) showed that the sonoCOF samples comprised sub-micron crystallites (Supplementary Figs. 25–42).

The permanent porosity of the sonoCOFs was assessed by nitrogen adsorption-desorption isotherms measured at 77 K after degassing at 120 °C for 12 h. For sonoCOF-1 and sonoCOF-2, the adsorption isotherms show characteristic type IV features (Supple-

mentary Figs 43a and 43b) with BET surface areas of 2059 and 1890 $m^2 g^{-1}$, respectively. For sonoCOF-3–7, the adsorption isotherms showed a rapid uptake at a low relative pressure of $P/P^0 < 0.01$ and reached saturation at $P/P^0 < 0.1$, which is characteristic of a type I isotherm for a microporous solid (Supplementary Figs 43c–43g). All sonoCOFs showed some hysteresis at higher pressures, likely due to the inter-particle mesoporosity formed from the aggregation of the COF nano-particles. Application of density functional theory (DFT) showed the pore size distribution of sonoCOFs-1–7 to be centred at ~3.17, 2.95, 1.84, 1.34, 2.40, 1.49 and 1.52 nm, respectively. The porosity of the sonoCOF (os) materials was measured under the same conditions as a control. All sonoCOFs exhibited higher BET surface areas and total pore volumes than their sonoCOF (os) analogs (Extended Data Fig. 1).

Comparison of literature BET surface areas and total pore volumes for the solvothermal analogs of these sonoCOFs showed similar or higher values for the sonoCOFs (Table 1) with one exception (sonoCOF-5). We note here that BET surface areas are sensitive to the relative pressure range used for the calculation. Also, the increase in total pore volume might be ascribed, at least in part, to inter-particle gas condensation for some of the sonoCOFs (*e.g.*, sonoCOF-3, see Supplementary Fig. 108), which typically comprise smaller microparticles than the analogous solvothermal materials.

Investigation of sonochemical COF formation. We next performed a series of control experiments to show that it is indeed sound energy that is driving these reactions. Reaction mixtures of the same composition used for sonoCOF-1-7 were treated under three different conditions:

Control-1: The amine and aldehyde monomers were added to an aqueous solution of acetic acid in a 4 mL vial and left at room temperature for 1 hour without stirring or sonication.

Control-2: The amine and aldehyde monomers were sonicated in aqueous acetic acid solution using a much less powerful standard laboratory ultrasonic cleaning bath at 25–38 °C for 1 hour, as opposed to using an ultrasonic probe.

Control-3: The amine and aldehyde monomers were stirred in an aqueous acetic acid solution at 80 °C in a heating block for 1 hour.

In Control-1, COFs were formed with significantly lower crystallinity and yield, except sonoCOF-2 and sonoCOF-3, which did not form at all under these conditions. The Control-2 and Control-3 conditions were more favorable, but again, products showed lower surface areas, lower total pore volumes and lower yields in all but one case. Notably, sonoCOF-3 did not form under any of the control conditions. These results are summarized in Supplementary Table 1.

Although sonocrystallization is known to lead to crystals with better uniformity, regularity, and less agglomeration in some cases, the mechanisms for these effects remain contentious because it is difficult to probe sonochemical processes on the time and length scales at which they occur.[41] Performing the reaction in aqueous acetic acid seems to be part of the reason for the high crystallinity and porosity observed, because the analogous reactions in mixtures of organic solvent and acetic acid were, in general, less successful. Certainly, water plays an important role during imine COF formation and other reports have shown that it aids COF crystallization.[42-44] We note for reaction mixtures in aqueous acetic acid, the amine monomers, with the exception of TAPT, were found to be highly soluble owing to protonation by acetic acid; by contrast, the aldehyde monomers were found to be sparingly soluble. As such, we believe that the COF reaction occurs under monomer starved conditions, but that formation and precipitation of the COF shifts the equilibrium, allowing more monomer to dissolve.

Our results do not agree with the conclusions of Thote *et al.*[16] and Martín-Illán *et al.*[18] who suggest that it is not possible to obtain imine-based COFs in high concentration aqueous AcOH solutions due to the protonation of the amine monomers. Our results clearly show that COFs can be formed under such conditions, at least when using sonochemistry.

Discovery of COFs. Having developed a robust method for the synthesis of seven known 2D COFs, we attempted the synthesis of two unreported COFs: a 2D COF with pendant functionalization, and a COF with 3D connectivity (Fig. 4). SonoCOF-8 is constructed from a chirally-functionalized building block TPB2,[45] forming an isostructural backbone to the TFB-TAPB COF 'RT-COF-1',[29] while sonoCOF-9 is a 3D COF based on the substitution of TFPB with TFPT in the family of 3D ETTA-containing COFs.[46] Formation of sonoCOF-8 and sonoCOF-9 was corroborated by FT-IR and CP-MAS ^{13}C NMR spectroscopies (see Supporting Information, section 3.2 and 3.8).

PXRD measurements for sonoCOF-8 (Fig. 3h) and sonoCOF-9 (Fig. 3i) showed diffraction peaks that were consistent with their simulated structures. The experimental PXRD pattern for sonoCOF-8 matched well with a simulated eclipsed AA-stacking arrangement (Supplementary Fig. 17). SonoCOF-9 exhibits good crystallinity with intense and sharp low-angle reflections, displaying a diffraction pattern very similar to the isostructural 3D-ETTA-TFPB COF.[46] However, rather than the previously reported phase 3D-ETTA-TFPB COF, we found that our diffraction data matched better with a monoclinic structure that we simulated with the **ffc** net (Supplementary Fig. 18). The crystal structure of sonoCOF-9 was assigned to the space group *Cm* with unit cell parameters of a = 74.42 Å, b = 43.95 Å, c = 23.44 Å, β = 89.89°.

Both sonoCOFs possessed permanent porosity, as shown by nitrogen adsorption-desorption isotherms measured at 77 K (Supplementary Fig. 43). The BET surface area was calculated to be 154 $m^2 g^{-1}$ for sonoCOF-8 and 984 $m^2 g^{-1}$ for sonoCOF-9, with total pore volumes of 0.19 and 0.52 $cm^3 g^{-1}$ at $P/P^0 = 0.97$ for sonoCOF-8 and sonoCOF-9, respectively.

Photocatalytic H_2 evolution. Recently, COFs have prompted interest as heterogeneous catalysts for photocatalytic water splitting.[47] Since high crystallinity is thought to be favourable for photocatalytic performance,[47,48] we tested these sonoCOFs for sacrificial photocatalytic H_2 evolution.

Initially, the photocatalytic activities of the sonoCOFs were screened using a high throughput instrument (see Supporting Information Section 1). As shown in Fig. 5a, sonoCOF-3, sonoCOF-6, and sonoCOF-9 exhibited high efficiency for photocatalytic hydrogen evolution with ascorbic acid as the sacrificial electron donor.

The best performing catalyst, sonoCOF-3 was studied in more detail. In the presence of ascorbic acid as a sacrificial electron donor, with Pt as a co-catalyst, sonoCOF-3 gave H_2 evolution rates of up to 16.6 mmol $h^{-1} g^{-1}$ under visible light ($\lambda > 420$ nm, 300 W Xenon lamp) (Fig. 5b). This is one of the highest sacrificial hydrogen evolution rates reported for a COF (Table S13). An external quantum efficiency (EQE) of 3.71 % was determined for sonoCOF-3 at 420 nm (Fig. 5c); for comparison, 3.2 % was reported for FS-COF[47] at 420 nm and 0.44% for N_3-COF[49] at 450 nm. We also compared the photocatalytic performance of sonoCOF-3 with its solvothermal analog (solvoCOF-3) in longer-term photocatalysis experiments under visible light irradiation ($\lambda > 420$ nm) (Fig. 5b). Both COFs continue to show hydrogen evolution for 40 hours, but sonoCOF-3 maintains very high activity at the end of the run while the catalytic efficiency of solvoCOF-3 is reduced. The PXRD pattern for sonoCOF-3 catalyst showed that crystallinity was retained after long-term irradiation to a greater extent than for solvoCOF-3 (Supplementary Fig. 102). In the course of this study, Thomas *et al*.[40] also reported high H_2 evolution rates using a COF ('TtaTfa' in their naming scheme) with the same chemical structure as sonoCOF-3. TfaTfa was synthesized using solvothermal conditions and the photocatalytic experiments were conducted under similar conditions. Degradation of catalytic activity and loss of crystallinity over longer-term photocatalysis was also observed for TtaTfa.

There are several microstructural differences between solvoCOF-3 and sonoCOF-3 that may contribute to the differences in their photocatalytic activity. Nitrogen adsorption porosimetry (Supplementary Figs 104-106) shows that sonoCOF-3 has a significantly higher BET surface area (1587 $m^2 g^{-1}$ compared with 1043 $m^2 g^{-1}$) and pore volume (1.04 $cm^3 g^{-1}$compared with 0.50 $cm^3 g^{-1}$) than solvoCOF-3, as well as a different pore-size distribution (Supplementary Fig 105). Although both samples show a bimodal distribution, the dominant pore size in sonoCOF-3 corresponds to the expected main pore (18.4 Å), while in solvoCOF-3 a smaller pore (15.2 Å) is overrepresented. This difference in pore distribution may arise from different concentrations of the stacking faults, as discussed previously. TEM images (Fig. 5) show that both sonoCOF-3 and solvoCOF-3 form rectangular particles, but the sonoCOF-3 particles are around half the length and width (~50×100 nm compared with ~100×200 nm); they are also thinner. In general, larger surface-to-volume ratios, as well as increased internal surface area, are expected to correlate with increased catalytic activity, particularly if the platinum cocatalyst is located on the surface of the COF particles, rather than in their pores.[48] Despite their smaller size, the sonoCOF-3 crystallites are well defined and highly crystalline, as evidenced by the HRTEM images. It is possible that the high crystallinity of the sonoCOF-3 particles or a greater degree of polymerization (Supplementary Fig. 107) enhances their resistance to thermal degradation, which is one possible explanation for their sustained hydrogen production. SonoCOF-3 also exhibits greater dispersibility in aqueous media (Supplementary Fig. 110), which is known to favor photocatalytic activity for materials of this type.[50] We also observed in several TEM images that the Pt co-catalyst appeared to be more evenly dispersed on the sonoCOF-3 particles (Supplementary Fig. 117), and improved resistance to Pt agglomeration will tend to enhance photocatalytic performance.

Conclusions

We present a rapid and clean method for COF synthesis using sonochemistry. Seven previously reported COFs and two new COFs were prepared. These materials were obtained in just 60 minutes by simply mixing and sonicating the reagents in water with acetic acid, and the products showed high porosity and high crystallinity. The temperature of the solutions increased during sonication, but control experiments with simple heating (Control 3; Supplementary Table 1) showed that the materials properties obtained are superior under sonication conditions. These sonochemical methods are more facile than conventional solvothermal syntheses, and this fast and convenient method is particularly suited to high-throughput discovery approaches.

Aqueous sonochemical synthesis has several advantages: the cost and toxicity of the process is reduced, and the need for solvent screening to optimize crystallinity is avoided. The functional properties of COFs can be improved through aqueous sonochemical routes, both in terms of porosity levels and other functional properties, such as photocatalytic activity. Moreover, the low reaction temperatures broaden the range of COF monomers that can be considered to encompass functionality that is thermally less stable, providing that is that these monomers can tolerate acidic conditions. We believe that sonochemical synthesis could be a powerful tool for the synthesis of COFs and that it deserves broader investigation for other functional materials, such as porous amorphous organic polymers, conjugated microporous polymers, or perhaps porous organic cages.

Methods

Synthesis of sonoCOFs via the sonochemical method. In a typical synthesis, the amine and aldehyde monomers are weighed into a 4 mL vial and aqueous acetic acid (2 mL) is then added. The mixture is sonicated using a 3 mm diameter microtip probe

driven by a 550 W Branson Sonifier SFX550 cell disrupter running at 20 kHz in continuous mode and at 50% power for 60 min. The resulting solids are washed in sequence with acetone, dichloromethane, and methanol, followed by a 24 h Soxhlet extraction with methanol. The sample is then dried under high vacuum for 24 h. For controls with organic solvents, the aqueous acid phase was replaced by the mixture of 1,4-dioxane (1 mL)/mesitylene (1 mL)/6M AcOH (0.2 mL) or n-BuOH (1 mL)/o-DCB (1 mL)/6M AcOH (0.2 mL).

Data availability

All data supporting the finding of this study are available within this article and its Supplementary Information. The experimental procedures and characterization of all COFs are provided in the Supplementary Information.

Acknowledgements

The authors acknowledge funding from the Leverhulme Trust via the Leverhulme Research Centre for Functional Materials Design and the Engineering and Physical Sciences Research Council (EPSRC). P.Y., H.C., L.L. and B.L. thank the China Scholarship Council for a PhD studentship. We thank the Materials Innovation Factory (MIF) team for help with instrument training. We thank Molly Lightowler of Stockholm University for testing the feasibility of using 3D electron diffraction to solve the COF structures. The TEM analysis was performed in the Albert Crewe Centre for Electron Microscopy, a University of Liverpool Shared Research Facility.

Author contributions

W.Z. synthesized and characterized the materials, performed photocatalytic experiments and analyzed the photocatalysis results with H.Y. P.Y. performed the SEM, TCSPC and FT-IR measurements. H.Y. performed the UV measurements. R.C. performed TGA measurements. A.M.J. and W.Z. performed gas adsorption measurements. H.C. and L.L. performed photoelectrochemical measurements. M.B. and N.D.B. performed TEM measurements. W.Z. conceived the modelling strategy. B.L. and Z.P. provided useful advice in the structural simulation of COFs. Y.W. and J.W.W. conceived the project. A.I.C., Y.W. and J.W.W directed the research. Data were interpreted by all authors and the manuscript was prepared by A.I.C., Y.W., J.W.W. and W.Z.

Competing interests

The authors declare no competing interests.

Tables

Table 1. Comparison of total pore volumes and BET surface areas of sonoCOFs with equivalent materials reported in the literature prepared under solvothermal conditions. SonoCOF reaction conditions: 60 min reaction time; reaction temperature starting at ambient temperature, ~20 ℃, and stabilizing at ~78 ℃after 10 minutes sonication, Supplementary Fig. 111. Literature reaction conditions: 120 ℃for 3–7 days. [a] Pore volume not reported. [b] Pore volume is calculated at $P/P^0 = 0.97$. [c] BET surface areas are calculated under P/P^0 =0.01–0.2 (see Supporting Information, Section 3.7).

SonoCOFs	Pore vol. ($cm^3\ g^{-1}$)	This work ($cm^3\ g^{-1}$) [b]	S_{BET} ($m^2\ g^{-1}$)	This work ($m^2\ g^{-1}$) [c]	Theoretical S_{BET} ($m^2\ g^{-1}$)	References
SonoCOF-1	1.28	1.80	2105	2059	2327	22
	1.28		1927			30
SonoCOF-2	1.59	1.45	1632	1890	2173	23
	– [a]		1314			31
	1.15		1036			32
SonoCOF-3	– [a]	1.04	1132	1587	1886	27
SonoCOF-4	0.56	0.67	1142	1425	1509	25
	0.66		1000			33
	0.55		1149			34
	0.55		1163			30
SonoCOF-5	1.09	1.51	2210	1746	1755	28
	– [a]		1520			26
	1.25		2039			35
SonoCOF-6	– [a]	0.81	1268	1013	1513	36
	– [a]		687			37
	– [a]		888			38
	– [a]		420			39
	0.44		435			34
SonoCOF-7	0.43	0.54	895	940	986	24

Figure captions

Figure 1. Apparatus and conditions used for sonochemical synthesis, the COFs studied, and the monomers used to synthesise them. (Left) Amine and aldehyde monomers used for COF synthesis. (Center) Schematic of the sonochemical apparatus and reaction setup. (Right) Structures of the COFs synthesised, their designations and their amine and aldehyde components.

Figure 2. Systematic investigation of the effect of reaction time on the prototypical COF 'TAPB-DMTA' formed by sonochemical synthesis ('SonoCOF-1') in aqueous acetic acid (a) Synthesis route for sonoCOF-1. (b) PXRD patterns show similar crystallinity regardless of reaction time. (c) N_2 adsorption isotherms show an increasing porosity at longer reaction times (d) FT-IR spectra show the presence of unreacted aldehyde at very short reaction times. All samples show the presence of the C=N bond, indicative of successful COF formation. (e) The yields (blue bars) and total pore volumes (pink bars) of sonoCOF-1 increase with greater reaction time.

Figure 3. The structures of sonoCOFs-1–9 confirmed by Pawley refinements based on modeled crystal structures. (a–i) Pawley refinements against the PXRD patterns of sonoCOF-1–9. Pink lines: y_{obs}, experimental PXRD data; black dots: y_{calc}, Pawley refinement profile; blue lines: $y_{obs} - y_{calc}$, residual; yellow marks: hkl positions calculated for that phase. Insets: Modeled crystal structures. C, grey; H, white; N, blue; O, red.

Figure 4. Synthetic routes for the unreported COFs sonoCOF-8 and sonoCOF-9. SonoCOF-8 contains a bulky pendant functional group, while sonoCOF-9 is the only sonoCOF with a 3D connectivity.

Figure 5. Photocatalytic hydrogen evolution experiments and characterization of sonoCOFs. (a) Screening of sonoCOFs for sacrificial photocatalytic hydrogen evolution. Conditions: 2 mg of COF catalyst, 16 μL H_2PtCl_6 solution (0.8 wt % in water), 5 mL 0.1 M ascorbic acid as a sacrificial electron donor, 2 h solar simulator illumination. Blue bars = aqueous sonoCOFs; pink bars = organic sonoCOFs (os). (b) Plot showing sacrificial photocatalytic hydrogen evolution as a function of time for sonoCOF-3 and solvoCOF-3 over 40 h (5 mg catalyst in water, diluted H_2PtCl_6 solution as a platinum precursor (4 wt % loading), 0.1 M ascorbic acid (25 ml), $\lambda > 420$ nm). The sample was degassed after 5 h and 10 h to prevent saturation of the detector, then left under continuous illumination for 15 h and again degassed after 30 h and 35 h. After 30 h, 1.25 mmol of ascorbic acid was added. (c) Overlay of the UV/vis absorption spectrum of sonoCOF-3 with external quantum efficiency (EQE) for the photocatalytic hydrogen evolution reaction with sonoCOF-3 at two different incident light wavelengths. (d) TEM images of solvoCOF-3 and sonoCOF-3 before and after photocatalytic testing and (e) HRTEM image of sonoCOF-3 clearly showing the hexagonal pore structure of a single crystallite.

References

1 Wang, Z., Zhang, S., Chen, Y., Zhang, Z. & Ma, S. Covalent organic frameworks for separation applications. *Chem. Soc. Rev*. **49**, 708-735 (2020).

2 Rodríguez-San-Miguel, D., Montoro, C. & Zamora, F. Covalent organic framework nanosheets: preparation, properties and applications. *Chem. Soc. Rev*. **49**, 2291-2302 (2020).

3 Song, Y., Sun, Q., Aguila, B. & Ma, S. Opportunities of covalent organic frameworks for advanced applications. *Adv. Sci.* **6**, 1801410 (2019).

4 Geng, K. Y. et al. Covalent organic frameworks: design, synthesis, and functions. *Chem. Rev*. **120**, 8814-8933 (2020).

5 Campbell, N. L., Clowes, R., Ritchie, L. K. & Cooper, A. I. Rapid microwave synthesis and purification of porous covalent organic frameworks. *Chem. Mater*. **21**, 204-206 (2009).

6 Matsumoto, M. et al. Rapid, low temperature formation of imine-linked covalent organic frameworks catalyzed by metal triflates. *J. Am. Chem. Soc*. **139**, 4999-5002 (2017).

7 Zhu, D. et al. Rapid, ambient temperature synthesis of imine covalent organic frameworks catalyzed by transition-metal nitrates. *Chem. Mater*. **33**, 3394-3400 (2021).

8 Kandambeth, S. et al. Selective molecular sieving in self-standing porous covalent-organic-framework membranes. *Adv. Mater*. **29**, 1603945 (2017).

9 Karak, S. et al. Constructing ultraporous covalent organic frameworks in seconds via an organic terracotta process. *J. Am. Chem. Soc*. **139**, 1856-1862 (2017).

10 Karak, S., Kumar, S., Pachfule, P. & Banerjee, R. Porosity prediction through hydrogen bonding in covalent organic frameworks. *J. Am. Chem. Soc*. **140**, 5138-5145 (2018).

11 Biswal, B. P. et al. Mechanochemical synthesis of chemically stable isoreticular covalent organic frameworks. *J. Am. Chem. Soc*. **135**, 5328-5331 (2013).

12 Das, G., Shinde, D. B., Kandambeth, S., Biswal, B. P. & Banerjee, R. Mechanosynthesis of imine, β-ketoenamine, and hydrogen-bonded imine-linked covalent organic frameworks using liquid-assisted grinding. *Chem. Commun*. **50**, 12615-12618 (2014).

13 Emmerling, S. T. et al. In situ monitoring of mechanochemical covalent organic framework formation reveals templating effect of liquid additive. *Chem* **7**, 1639-1652(2021).

14 Feriante, C. H. et al. Rapid synthesis of high surface area imine-linked 2D covalent organic frameworks by avoiding pore collapse during isolation. *Adv. Mater*. **32**, 1905776 (2019).

15 Sick, T. et al. Switching on and off interlayer correlations and porosity in 2D covalent organic frameworks. *J. Am. Chem. Soc*. **141**, 12570-12581 (2019).

16 Thote, J. et al. Constructing covalent organic frameworks in water via dynamic covalent bonding. *IUCrJ*. **3**, 402-407 (2016).
17 Lu, J. et al. Large-scale synthesis of azine-linked covalent organic frameworks in water and promoted by water. *New J. Chem*. **43**, 6116-6120 (2019).
18 Martín-Illán, J. Á. et al. Green synthesis of imine-based covalent organic frameworks in water. *Chem. Commun*. **56**, 6704-6707 (2020).
19 Suslick, K. S. Sonochemistry. *Science* **247**, 1439-1445 (1990).
20 Yang, S. T., Kim, J., Cho, H. Y., Kim, S. & Ahn, W. S. Facile synthesis of covalent organic frameworks COF-1 and COF-5 by sonochemical method. *RSC Adv*. **2**, 10179 (2012).
21 Yoo, J. et al. In situ synthesis of covalent organic frameworks (COFs) on carbon nanotubes and graphenes by sonochemical reaction for CO_2 adsorbents. *Chem. Lett*. **44**, 560-562 (2015).
22 Xu, H., Gao, J. & Jiang, D. L. Stable, crystalline, porous, covalent organic frameworks as a platform for chiral organocatalysts. *Nat. Chem*. **7**, 905-912 (2015).
23 Zhi, Y. F. et al. Covalent organic frameworks as metal-free heterogeneous photocatalysts for organic transformations. *J. Mater. Chem. A* **5**, 22933-22938 (2017).
24 Nguyen, H. L. et al. A porous covalent organic framework with voided square grid topology for atmospheric water harvesting. *J. Am. Chem. Soc*. **142**, 2218-2221 (2020).
25 Bai, L. Y., Gao, Q. & Zhao, Y. L. Two fully conjugated covalent organic frameworks as anode materials for lithium ion batteries. *J. Mater. Chem. A* **4**, 14106-14110 (2016).
26 Ascherl, L. et al. Solvatochromic covalent organic frameworks. *Nat. Commun*. **9**, 3802 (2018).
27 EL-Mahdy, A. F. M. et al. Strategic design of triphenylamine- and triphenyltriazine-based two-dimensional covalent organic frameworks for CO_2 uptake and energy storage. *J. Mater. Chem. A* **6**, 19532-19541 (2018).
28 Auras, F. et al. Synchronized offset stacking: A concept for growing large-domain and highly crystalline 2D covalent organic frameworks. *J. Am. Chem. Soc*. **138**, 16703-16710 (2016).
29 de la Peña Ruigómez, A. et al. Direct on-surface patterning of a crystalline laminar covalent organic framework synthesized at room temperature. *Chem. Eur. J*. **21**, 10666-10670 (2015).
30 Wang, P. et al. Exceptional iodine capture in 2D covalent organic frameworks. *Adv. Mater*. **30**, 1801991 (2018).
31 Zhu, D. & Verduzco, R. Ultralow surface tension solvents enable facile COF activation with reduced pore collapse. *ACS Appl. Mater. Interfaces* **12**, 33121-33127 (2020).
32 Mullangi, D. et al. Highly stable COF-supported $Co/Co(OH)_2$ nanoparticles heterogeneous catalyst for reduction of nitrile/nitro compounds under mild conditions. *Small* **14**, 1801233 (2018).
33 Bai, L. et al. Nanoscale covalent organic frameworks as smart carriers for drug delivery. *Chem. Commun*. **52**, 4128-4131 (2016).
34 Dong, J., Wang, Y., Liu, G., Cheng, Y. & Zhao, D. Isoreticular covalent organic frameworks for hydrocarbon uptake and separation: the important role of monomer planarity. *CrystEngComm* **19**, 4899-4904 (2017).
35 Meng, Y., Lin, G., Ding, H., Liao, H. & Wang, C. Impregnation of sulfur into a 2D pyrene-based covalent organic framework for high-rate lithium-sulfur batteries. *J. Mater. Chem. A* **6**, 17186-17191 (2018).
36 Li, X. et al. Molecular engineering of bandgaps in covalent organic frameworks. *Chem. Mater*. **30**, 5743-5749 (2018).
37 Shan, Z. et al. Dynamic transformation between covalent organic frameworks and discrete organic cages. *J. Am. Chem. Soc*. **142**, 21279-21284 (2020).
38 Romero Muñiz, I. et al. Unveiling the local structure of palladium loaded into imine-linked layered covalent organic frameworks for cross-coupling catalysis. *Angew. Chem. Int. Ed*. **59**, 13013-13020 (2020).
39 Garzón Tovar, L. et al. A MOF@COF composite with enhanced uptake through interfacial pore generation. *Angew. Chem. Int. Ed*. **58**, 9512-9516 (2019).
40 Yang, J. et al. Protonated imine-linked covalent organic frameworks for photocatalytic hydrogen evolution. *Angew. Chem. Int. Ed*. **60**, 19797-19803 (2021).
41 Nalesso, S., Bussemaker, M. J., Sear, R. P., Hodnett, M. & Lee, J. A review on possible mechanisms of sonocrystallisation in solution. *Ultrason. Sonochem*. **57**, 125-138 (2019).
42 Smith, B. J., Overholts, A. C., Hwang, N. & Dichtel, W. R. Insight into the crystallization of amorphous imine-linked polymer networks to 2D covalent organic frameworks. *Chem. Commun*. **52**, 3690-3693 (2016).
43 Li, H. et al. Nucleation and growth of covalent organic frameworks from solution: The example of COF-5. *J. Am. Chem. Soc*. **139**, 16310-16318 (2017)
44 Stewart, D. et al. Stable and ordered amide frameworks synthesised under reversible conditions which facilitate error checking. *Nat. Commun*. **8**, 1102 (2017).
45 Zhang, J., Han, X., Wu, X., Liu, Y. & Cui, Y. Multivariate chiral covalent organic frameworks with controlled crystallinity and stability for asymmetric catalysis. *J. Am. Chem. Soc*. **139**, 8277-8285 (2017).
46 Lan, Y. et al. Materials genomics methods for high-throughput construction of COFs and targeted synthesis. *Nat. Commun*. **9**, 5274 (2018).
47 Wang, X. et al. Sulfone-containing covalent organic frameworks for photocatalytic hydrogen evolution from water. *Nat. Chem*. **10**, 1180-1189 (2018).
48 Aitchison, C. M. et al. Photocatalytic proton reduction by a computationally identified molecular hydrogen-bonded framework. *J. Mater. Chem. A* **8**, 7158-7170 (2020).
49 Vyas, V. S. et al. A tunable azine covalent organic framework platform for visible light induced hydrogen generation. *Nat. Commun*. **6**, 8508(2015).
50 Bai, Y. et al. Accelerated discovery of organic polymer photocatalysts for hydrogen evolution from water through the in-

tegration of experiment and theory. *J. Am. Chem. Soc*. **141**, 9063-9071 (2019).

Amines

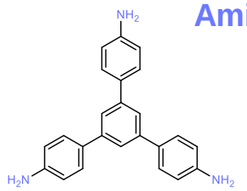

TAPB

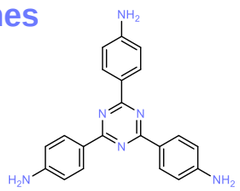

TAPT

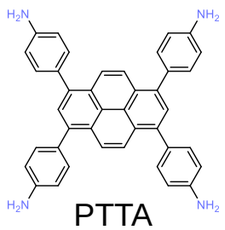

PTTA

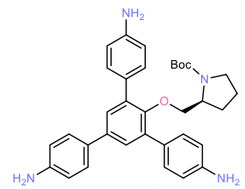

TPB2

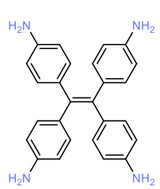

ETTA

Aldehydes

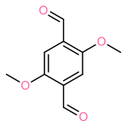

DMTA

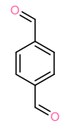

TPA

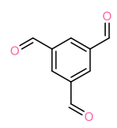

TFB

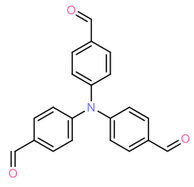

TFPA

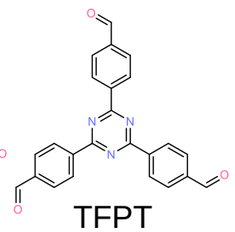

TFPT

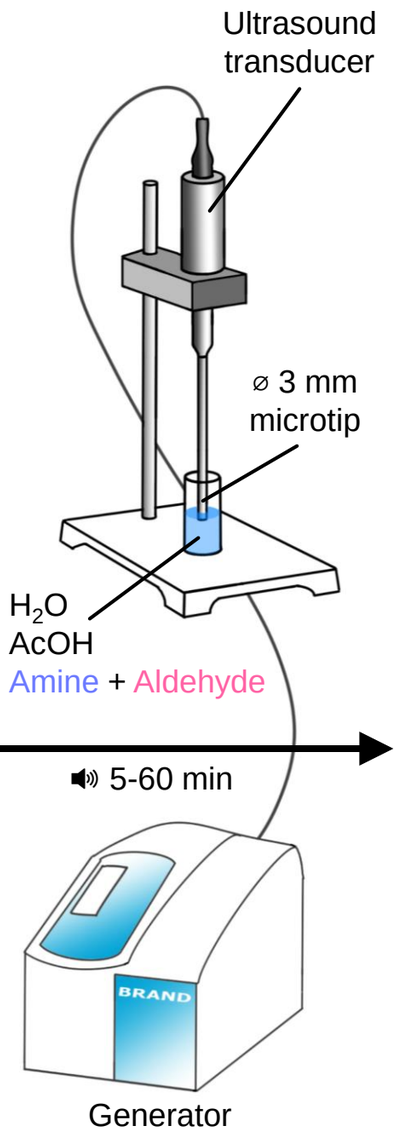

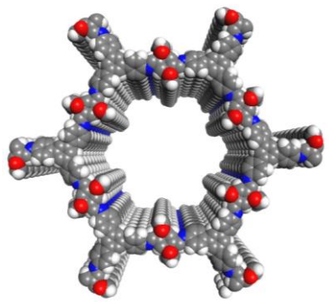

SonoCOF-1
TAPB-DMTA

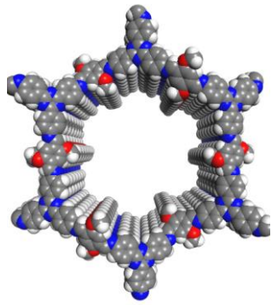

SonoCOF-2
TAPT-DMTA

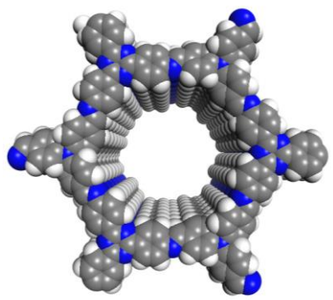

SonoCOF-3
TAPT-TFPA

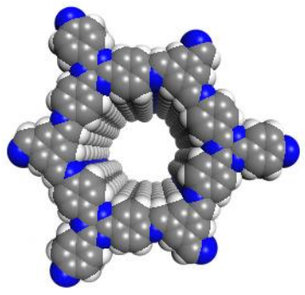

SonoCOF-4
TAPT-TFB

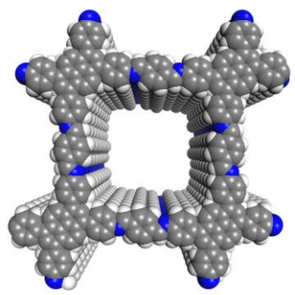

SonoCOF-5
PTTA-TPA

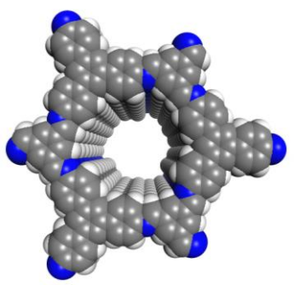

SonoCOF-6
TAPB-TFB

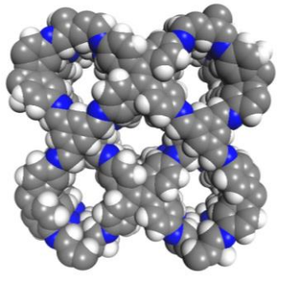

SonoCOF-7
ETTA-TFB

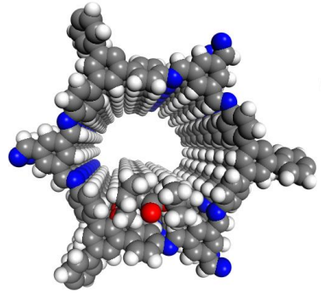

SonoCOF-8
TPB2-TFB

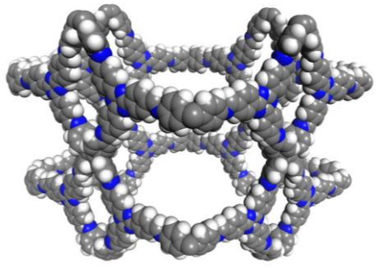

SonoCOF-9
ETTA-TFPT

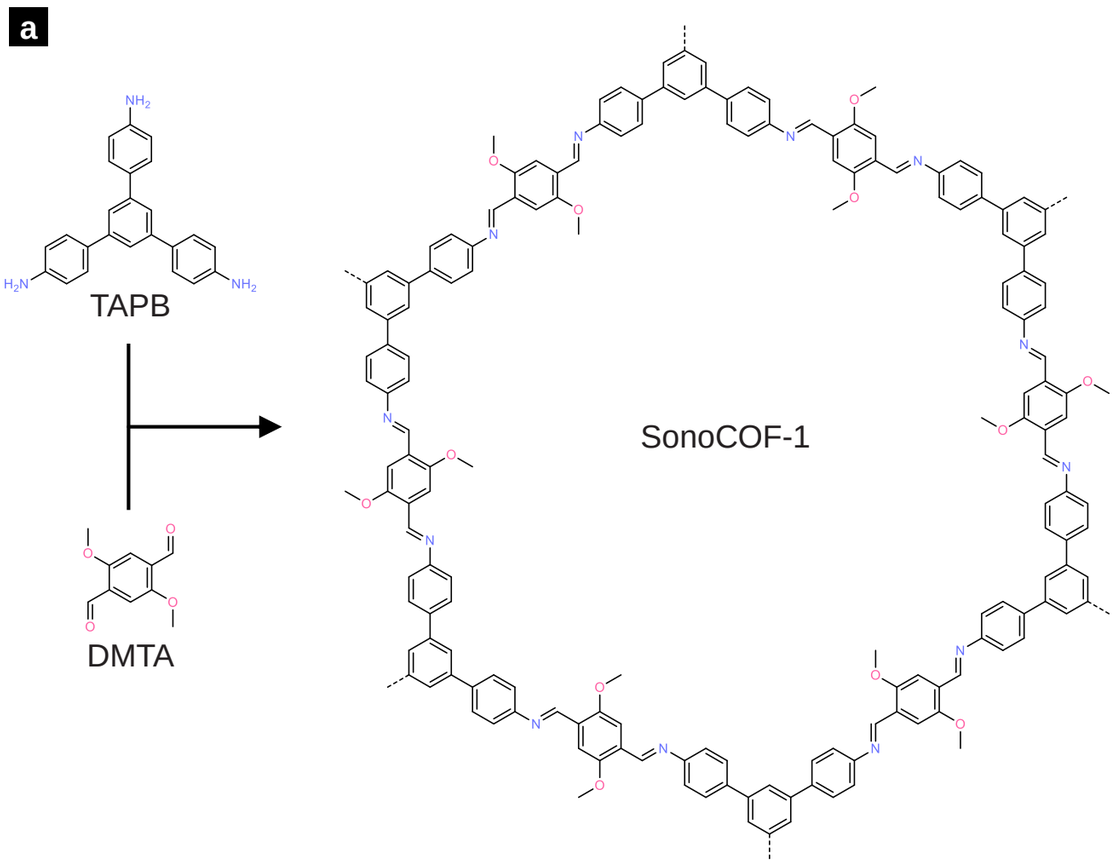
a
TAPB
DMTA
SonoCOF-1

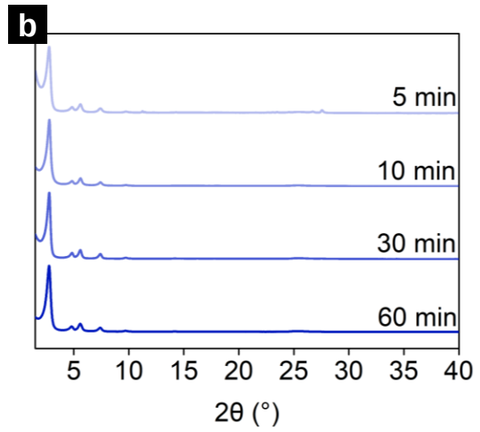
b
5 min
10 min
30 min
60 min
2θ (°)

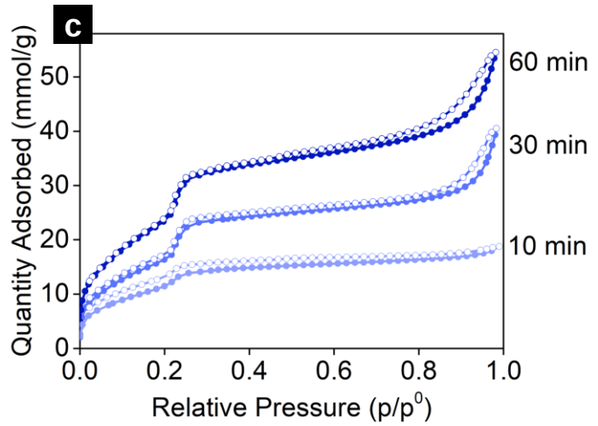
c
Quantity Adsorbed (mmol/g)
60 min
30 min
10 min
Relative Pressure (p/p0)

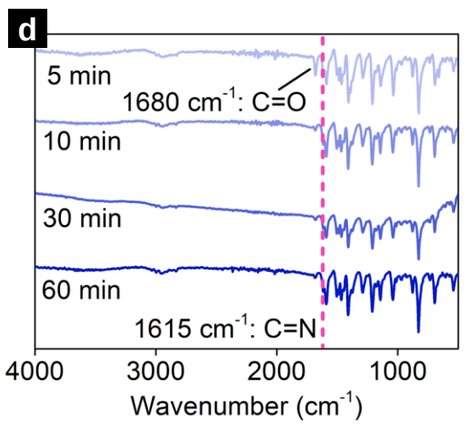
d
5 min
1680 cm-1: C=O
10 min
30 min
60 min
1615 cm-1: C=N
Wavenumber (cm-1)

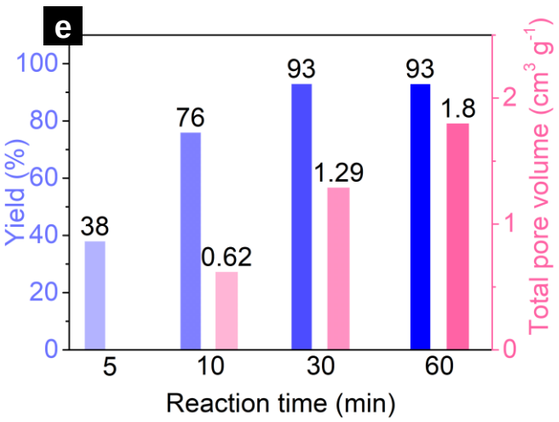
e
Yield (%)
Total pore volume (cm3 g-1)
38
76
0.62
93
1.29
93
1.8
Reaction time (min)

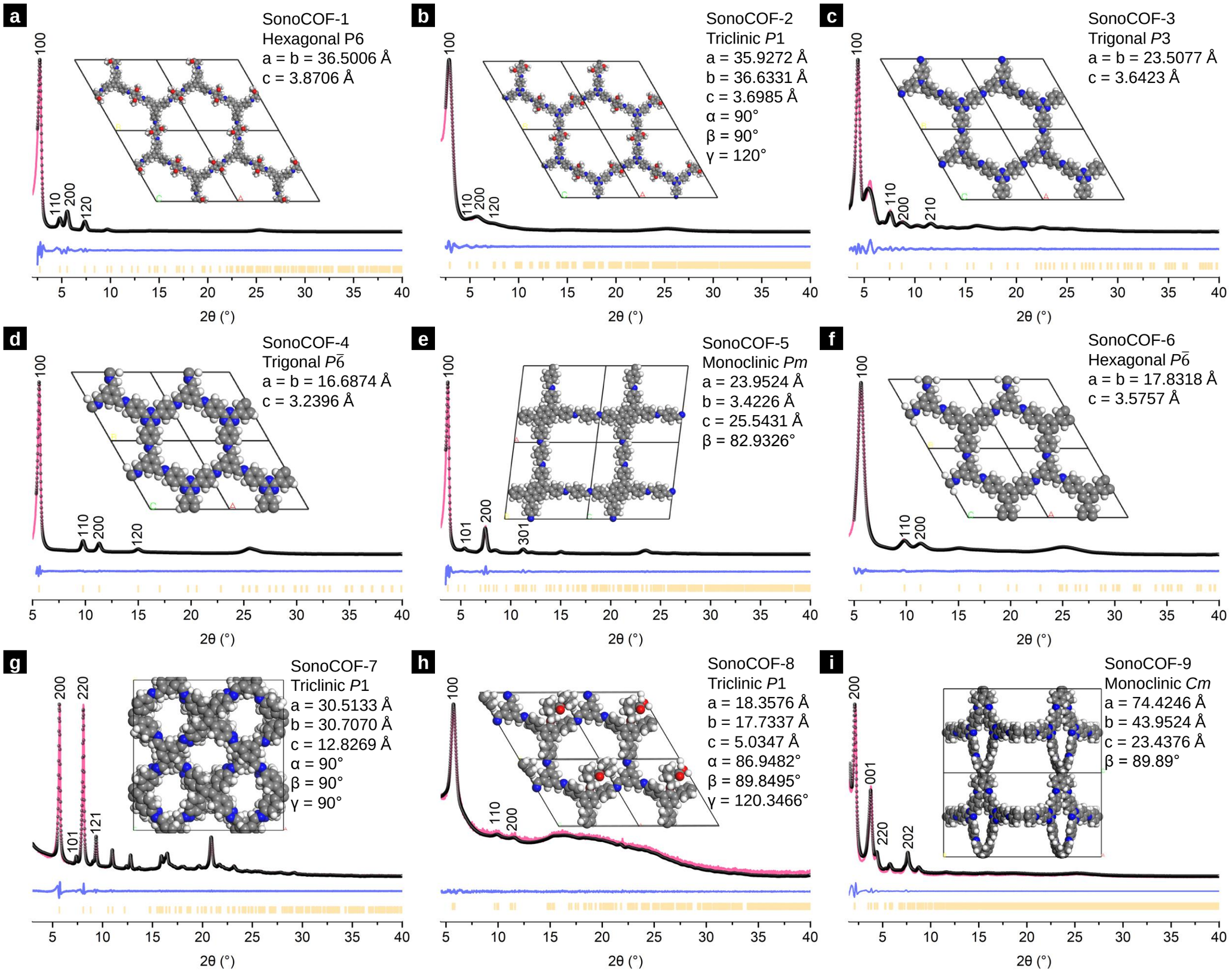
a
SonoCOF-1
Hexagonal P6
a = b = 36.5006 Å
c = 3.8706 Å
100
110
200
120
b
SonoCOF-2
Triclinic P1
a = 35.9272 Å
b = 36.6331 Å
c = 3.6985 Å
α = 90°
β = 90°
γ = 120°
100
110
200
120
c
SonoCOF-3
Trigonal P3
a = b = 23.5077 Å
c = 3.6423 Å
100
110
200
210
d
SonoCOF-4
Trigonal P6̄
a = b = 16.6874 Å
c = 3.2396 Å
100
110
200
120
e
SonoCOF-5
Monoclinic Pm
a = 23.9524 Å
b = 3.4226 Å
c = 25.5431 Å
β = 82.9326°
100
101
200
301
f
SonoCOF-6
Hexagonal P6̄
a = b = 17.8318 Å
c = 3.5757 Å
100
110
200
g
SonoCOF-7
Triclinic P1
a = 30.5133 Å
b = 30.7070 Å
c = 12.8269 Å
α = 90°
β = 90°
γ = 90°
200
220
101
121
h
SonoCOF-8
Triclinic P1
a = 18.3576 Å
b = 17.7337 Å
c = 5.0347 Å
α = 86.9482°
β = 89.8495°
γ = 120.3466°
100
110
200
i
SonoCOF-9
Monoclinic Cm
a = 74.4246 Å
b = 43.9524 Å
c = 23.4376 Å
β = 89.89°
200
001
220
202
5
10
15
20
25
30
35
40
2θ (°)

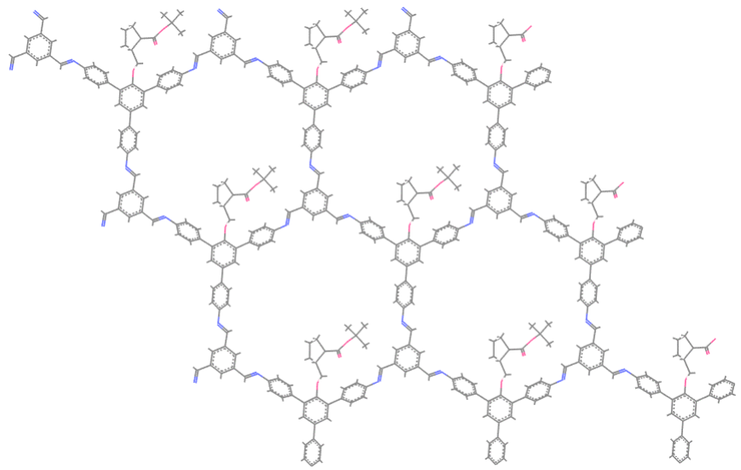

SonoCOF-8

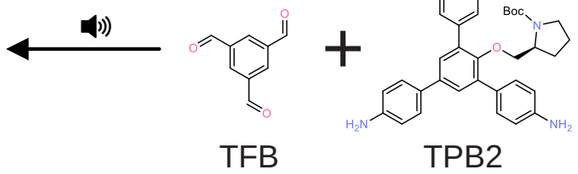

TFB

TPB2

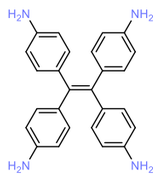

ETTA

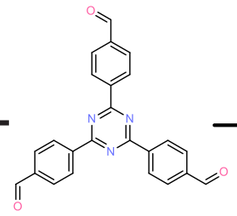

TFPT

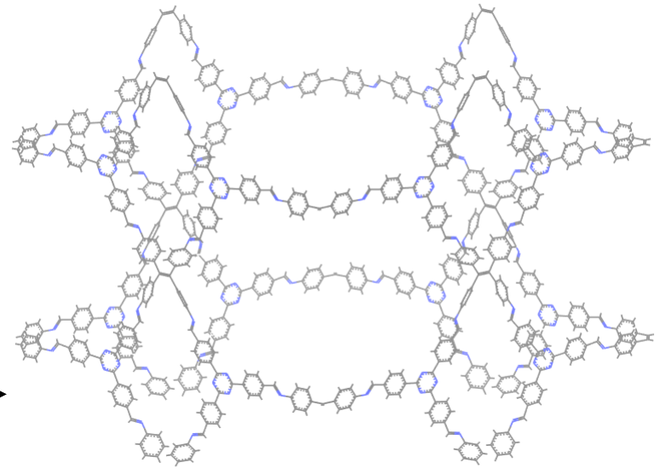

SonoCOF-9

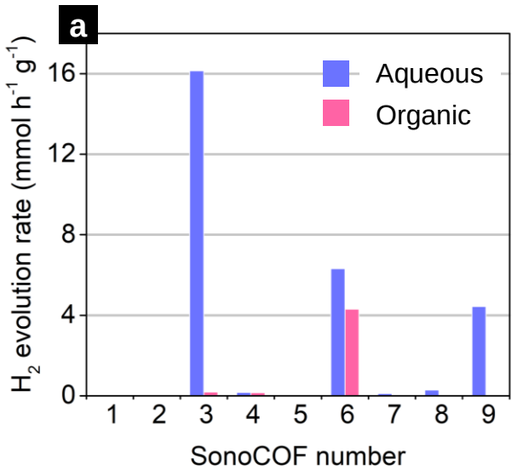
a
Aqueous
Organic
H2 evolution rate (mmol h-1 g-1)
SonoCOF number

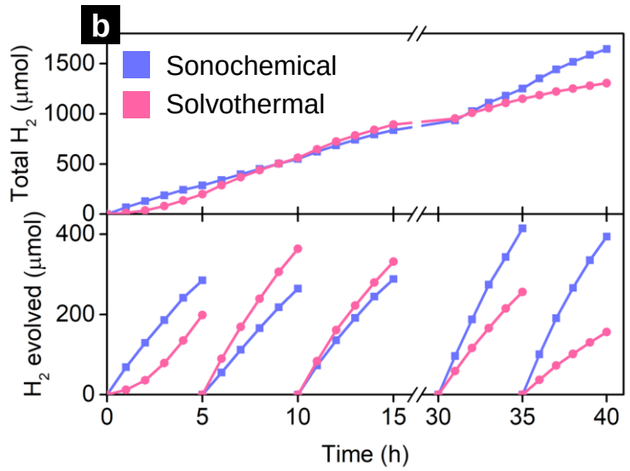
b
Sonochemical
Solvothermal
Total H2 (μmol)
H2 evolved (μmol)
Time (h)

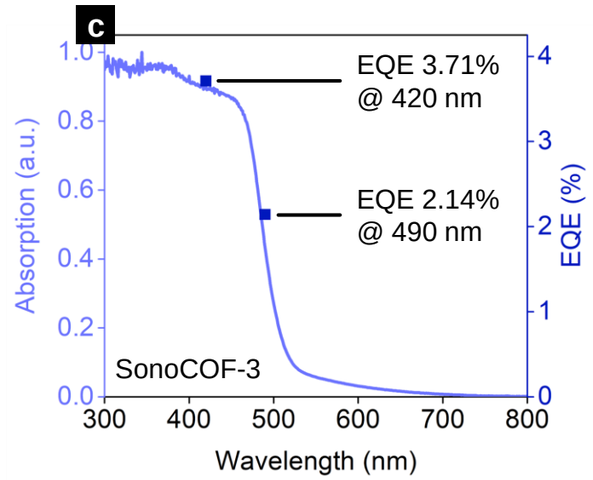
c
EQE 3.71%
@ 420 nm
EQE 2.14%
@ 490 nm
SonoCOF-3
Absorption (a.u.)
EQE (%)
Wavelength (nm)

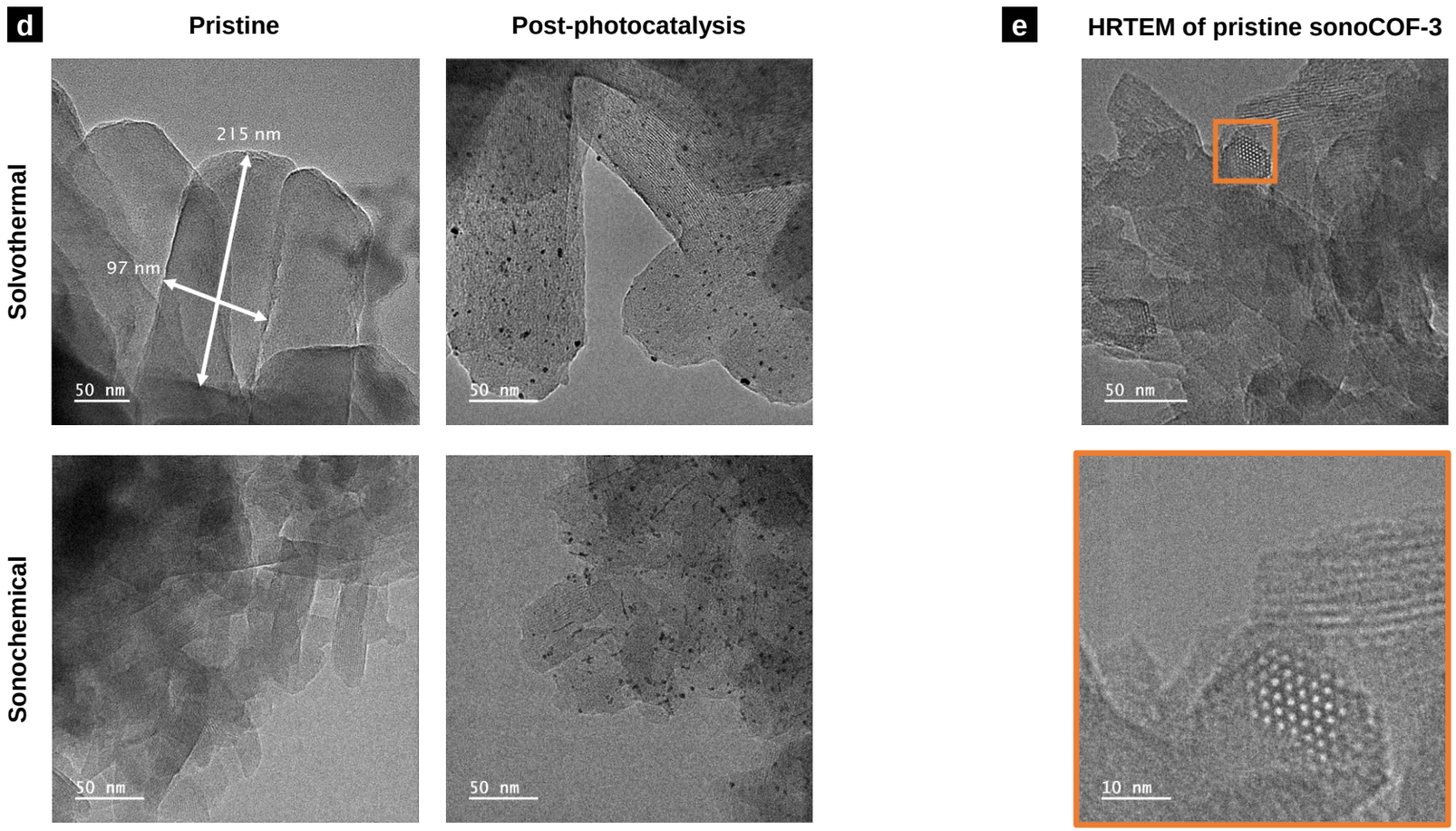
d
Pristine
Post-photocatalysis
Solvothermal
Sonochemical
215 nm
97 nm
50 nm
e
HRTEM of pristine sonoCOF-3
10 nm

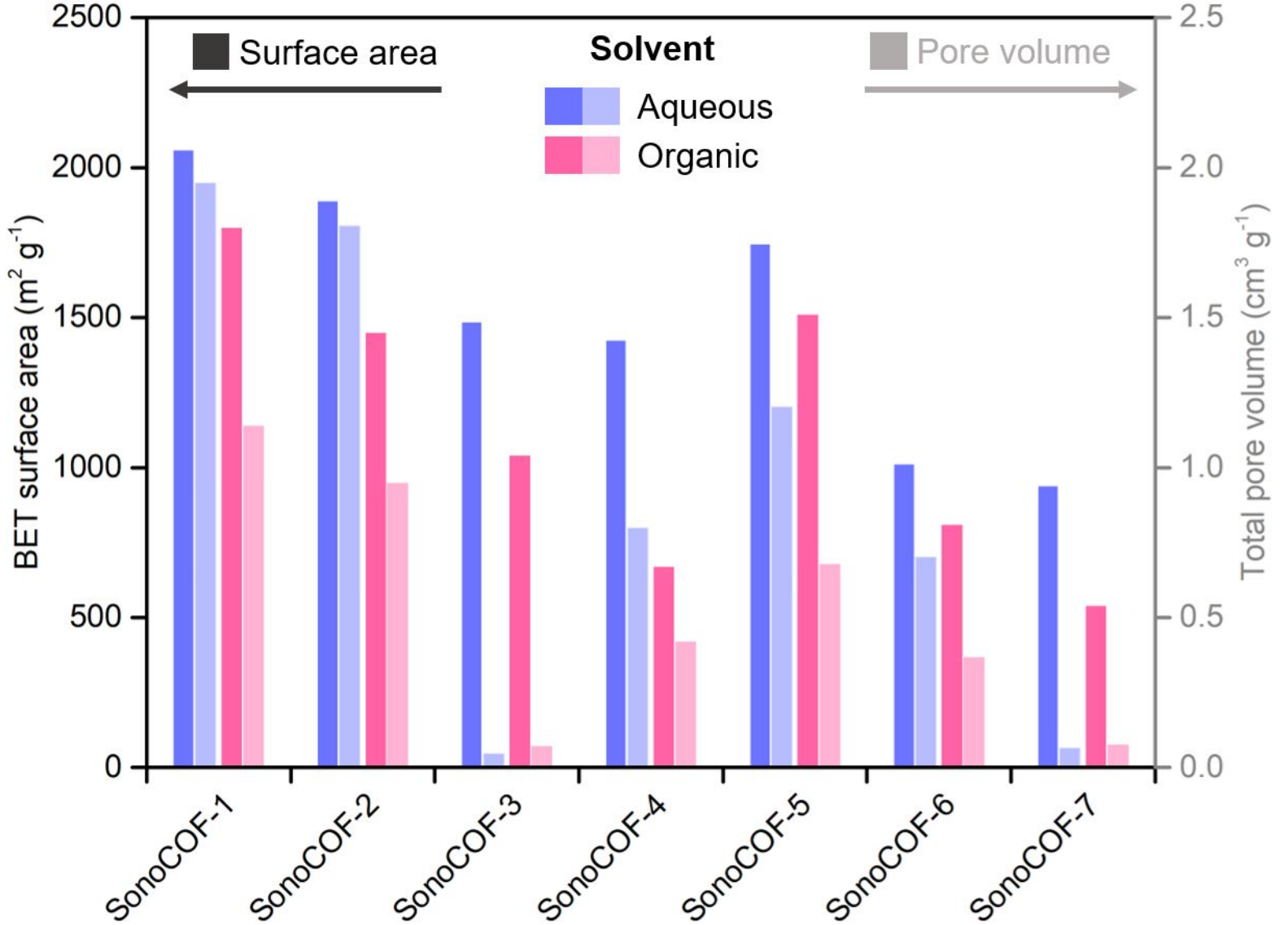
Surface area
Solvent
Aqueous
Organic
Pore volume
BET surface area (m2 g-1)
Total pore volume (cm3 g-1)
2500
2000
1500
1000
500
0
2.5
2.0
1.5
1.0
0.5
0.0
SonoCOF-1
SonoCOF-2
SonoCOF-3
SonoCOF-4
SonoCOF-5
SonoCOF-6
SonoCOF-7

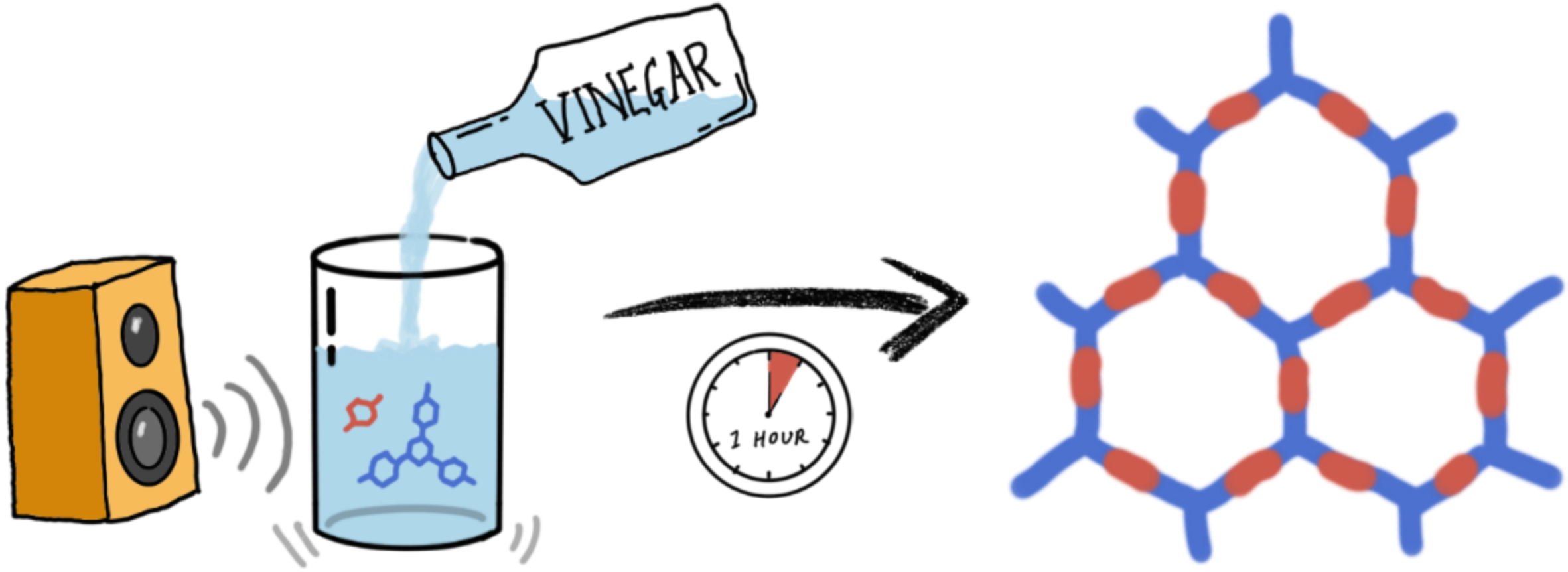

Aqueous sonochemical COF synthesis